Pis'ma v ZhETF, vol. 88, iss. 5, pp. 360 – 365 

# Two-electron bound states in continuum in quantum dots

*A. F. Sadreev, T. V. Babushkina*[+]

*Institute of Physics RAS, 660036 Krasnoyarsk, Russia*

[+]*Siberian Federal University, 660079 Krasnoyarsk, Russia*

Submitted 4 May 2008
Resubmitted 16 July 2008

Bound state in continuum (BIC) might appear in open quantum dots for variation of the dot's shape. By means of the equations of motion of Green functions we investigate effect of strong intradot Coulomb interactions on that phenomenon in the framework of impurity Anderson model. Equation that imaginary part of poles of the Green function equals to zero gives condition for BICs. As a result we show that Coulomb interactions replicate the single-electron BICs into two-electron ones.

PACS: 05.60.Gg, 71.27.+a, 72.10.–d, 73.23.Hk

In 1929, von Neumann and Wigner [1] predicted the existence of discrete solutions of the single-particle Schrödinger equation embedded in the continuum of positive energy states. Their analysis examined by Stillinger and Herrick [2] long time was regarded as mathematical curiosity because of certain spatially oscillating central symmetric potentials. More recently in 1973 Herrik [3] and Stillinger [4] predicted BICs in semiconductor heterostructure superlattices which were observed by Capasso et al. as the very narrow absorption peak [5].

In the framework of the Feshbach's theory of resonances Friedrich and Wintgen [6] have shown that bound state in continuum (BIC) occurs due to the interference of resonances. If two resonances pass each other as a function of a continuous parameter, then for a given value of the parameter one resonance has exactly vanishing width. Later this result was reproduced in application to different physical systems in the two-level approximation [7 – 12]. Straight waveguide with an attractive, finite size impurity presents an example of realistic structure in which Kim et al. presented the numerical evidence for the BIC for the variation of the impurity size [13]. Further, calculations in microwave and semiconductor open structures showed that the resonance width also can turn to zero for variation of angle of bent waveguide [14], shape of quantum dot (or resonator) [12, 15], or magnetic field [16]. Recently it was rigorously shown that the zero resonance width is the necessary and sufficient condition for BIC [16, 17]. This condition means that a coupling of the resonance state with continuum equals zero to convert the state into BIC [18, 16].

That very restricted list of references shows that BICs might occur in different open quantum systems including, for example, laser induced continuum structures in atoms [19], in the molecular system [20]. However in application to open quantum dots (QD) BICs were studied in the single electron approximation whereas the Coulomb interactions between electrons might be very important for robustness of the BIC. In the present work we consider effect of local intradot Coulomb interactions in QD onto BICs in the framework of the two-level impurity Anderson model [21] that is one of the most important theoretical models for a study of strong correlations in condensed matter physics.

We consider QD coupled to leads (left and right) which support one propagating mode (the case of two continuums) with the following total Hamiltonian

$$H = \sum_{C=L,R} H_C + H_D + V. \quad (1)$$

The leads, left $L$ and right $R$ in (1) are presented as the non interacting electron gas

$$H_C = \sum_{k\sigma} \epsilon(k) c^+_{k\sigma C} c_{k\sigma C}, \ C = L, R. \quad (2)$$

A continual spectrum $\epsilon(k)$ defines the propagating band of leads. The Hamiltonian of many level QD is that of the impurity Anderson model [21],

$$H_D = \sum_{m\sigma} \epsilon_m a^+_{m\sigma} a_{m\sigma} + \sum_m U_m n_{m\sigma} n_{m\overline{\sigma}}. \quad (3)$$

Here $a^+_{m\sigma}$ is the creation operator of an electron on the m-th level of QD, $U_m$ takes into account the Hubbard repulsion at the level $m$, and $n_{m\sigma} = a^+_{m\sigma} a_{m\sigma}$. The interaction

$$V = \sum_{k\sigma mC} V_m(k)(c^+_{k\sigma C} a_{m\sigma} + \text{h.c}) \quad (4)$$

describes couplings between the leads and QD where $c^{+}_{k\sigma C}$ is the creation operator of an electron in the lead $C$.

In order to calculate transport properties of the QD we use a technique of the equations of motion for retarded and advanced Green functions which successfully used to consider the Fano and Kondo resonances in the Anderson model [22–27]. Following Laxroix [28] we use a Hartree-Fock approximation in the wires $\langle\langle c_{k\sigma C} a^{+}_{n\overline{\sigma}} a_{n\overline{\sigma}} | a^{+}_{m\sigma'} \rangle\rangle \approx \langle n_{n\overline{\sigma}} \rangle \langle\langle c_{k\sigma C} | a^{+}_{m\sigma'} \rangle\rangle$. The approximation is justified for weak couplings compared to the Coulomb interactions: $V_m \ll U_m$. As a result we obtain the following equation

$$\mathbf{G}^{-1}(E) = \mathbf{G}^{-1}_{QD}(E) + i\Gamma \qquad (5)$$

for the Green functions $G_{m\sigma,n\sigma'}(E) = \langle\langle a_{m\sigma} | a^{+}_{n\sigma'} \rangle\rangle^{-1}$ in the form of the Dyson equation [24]. Here $\mathbf{G}_{QD}(E)$ is the Green function of the isolated QD

$$G_{QD,mm',\sigma,\sigma'}(E) = G_{QD,m\sigma}(E)\delta_{mm'}\delta_{\sigma,\sigma'},$$
$$G_{QD,m\sigma}(E) = \frac{1-\langle n_{m\overline{\sigma}}\rangle}{E-\epsilon_m} + \frac{\langle n_{m\overline{\sigma}}\rangle}{E-\epsilon_m-U_m}, \qquad (6)$$

which are exact for the isolated QD. For the simplicity we take wide band wires and approximate the self-energy as [29, 24]

$$\sum_k \frac{V_m(k)V_n(k)}{E-\epsilon(k)_\sigma + i0} = -i\pi V_m V_n \rho_C(E) = -i\sqrt{\Gamma_m\Gamma_n} \qquad (7)$$

where $\rho_C(E)$ is the density of states of the left and right wires. The average values of the occupation numbers $\langle n_{m\sigma}\rangle = \langle a^{+}_{m\sigma} a_{m\sigma}\rangle$ which enter the expressions for the Green functions are calculated self-consistently via the formulas [28]

$$\langle n_{m\sigma}\rangle = \frac{1}{\pi}\int dE\, \mathrm{Im} G_{m\sigma,m\sigma}(E). \qquad (8)$$

The form of the self-energy (7) and the QD Green function (6) allows to proceed to the case of free electrons with $U_m = 0$. In this case BIC appears if QD acquires accidental degeneracy $\epsilon_1 = \epsilon_2$ [12]. Therefore in the vicinity of the degeneracy point $\varepsilon = \epsilon_2 - \epsilon_1 = 0$ we can restrict ourselves to the two-level approximation for QD [9]. Then the occupation numbers (8) are given by four poles of the Green function (5). At zero temperature, the transmission amplitude can be expressed in term of the Green function

$$T = \Gamma G(E)\Gamma^{+},\ \Gamma = (\Gamma_1, \Gamma_2). \qquad (9)$$

The results of numerical self-consistent calculation of the transmission (9) are presented in Fig.1. Fig.1a shows the case of zero Hubbard repulsion $U_m = 0$ (no electron correlations) in which QD is given only by

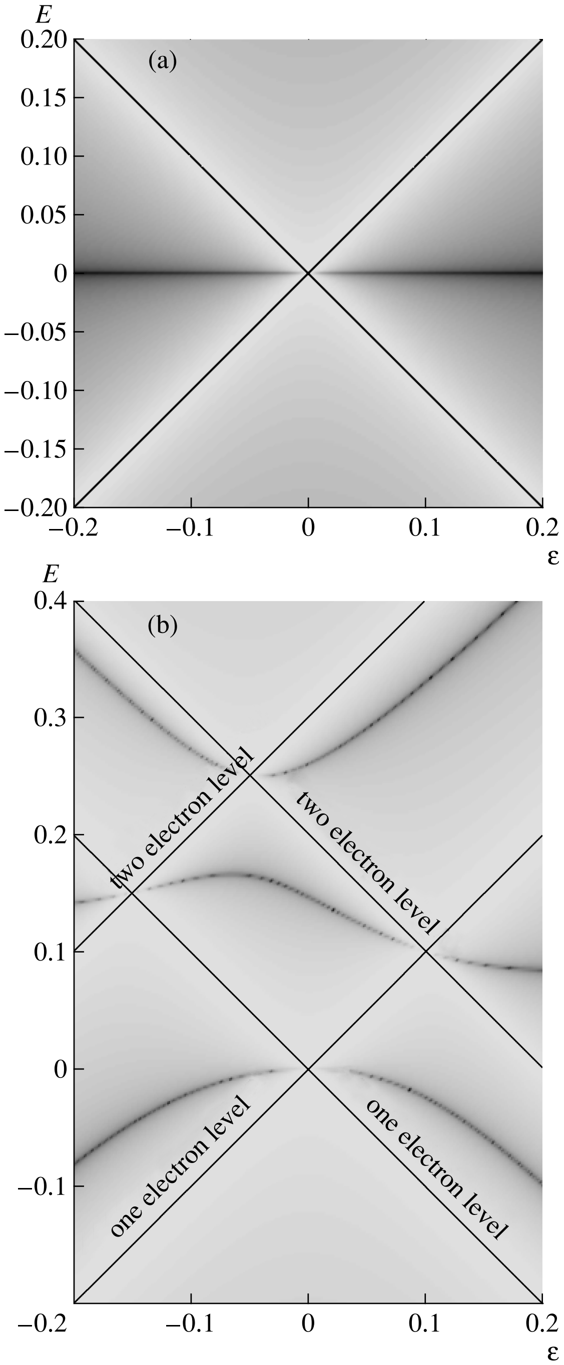


Fig.1. (a) The transmission $\ln|T|$ of QD versus energy of incident electron and energy splitting $\epsilon$ for the case of zero Hubbard repulsion $U_1 = U_2 = 0$. (b) The case of strong Hubbard repulsion $U_1 = 0.2$, $U_2 = 0.3, \Gamma_1 = \Gamma_2 = 0.05$. The single-electron and two-electron energy levels in closed QD are shown by thin lines. Black regions correspond to those where the transmission close to zero while the white regions do to the maximal transmission

the single-electron energy levels. As shown in [9, 12] BIC occurs here at the point of degeneracy of electron states in QD for $\epsilon = 0$. At this point the $S$-matrix becomes singular because the transmission zero crosses the unit transmission [12] as shown in Fig.1 where the unit transmission follows the energy levels. As the Hubbard repulsion is included, QD is given not only by single-electron states but also by two-electron states as shown in Fig.1b by solid lines. As a result we obtain that the number of degenerated points becomes four as seen from Fig.1b. One can see that lines of zero transmission cross the lines of maximal unit transmission at these points. Therefore, one can expect the BICs at four points of degeneracy of the QD. In order to show that we present in Fig.2 the resonance widths of the

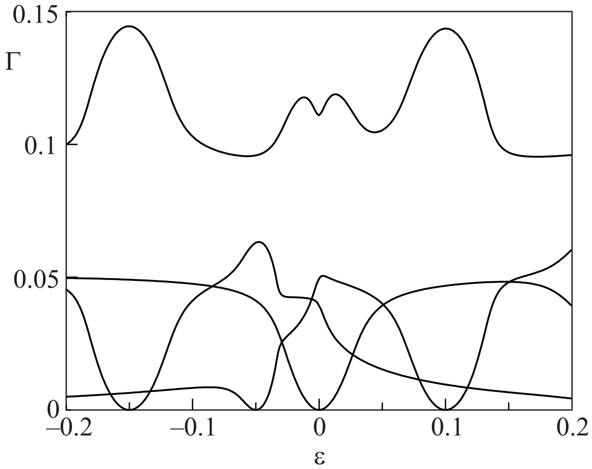


Fig.2. The resonance widths defined as $-2Im[z_\lambda(E,\epsilon)]$, $\lambda = 1,2,3,4$ versus $\epsilon$ for $E = 0$ where $z_\lambda$ are the poles of the Green function (5)

energy levels defined as $\Gamma_\lambda = -2\mathrm{Im}(z_\lambda)$, $\lambda = 1,2,3,4$, where $z_\lambda(E,\epsilon)$ are the poles of the Green function or zeros of the right hand expression in the Dyson equation (5). The points at which $\Gamma_\lambda = 0$ define BICs [16, 17]. One can see that these points coincide with the points of degeneracy of the QD given by equations $\epsilon_{c1} = 0$, $\epsilon_{c2} = U_1/2$, $\epsilon_{c3} = -U_2/2$, $\epsilon_{c4} = (U_2 - U_1)/2$. The corresponding energies of BICs are 0, 0.1, −0.15, 0.05. The first BIC is pure single electron localized state superposed of two single electron states with $m = 1,2$ [12]. However the next two BICs are supespositions of the single electron states and two-electron ones. At last, for the last case ($\epsilon_{c4} = (U_2 - U_1)/20$ the BIC is superposed of the two-electron states in QD. Although specific values of $\Gamma_m$ has no importance for BIC's points defined by crossings of the energy levels of QD, they are important for appearance of the Dicke superradiant state which accumulates the total width [9] as seen from Fig.2.

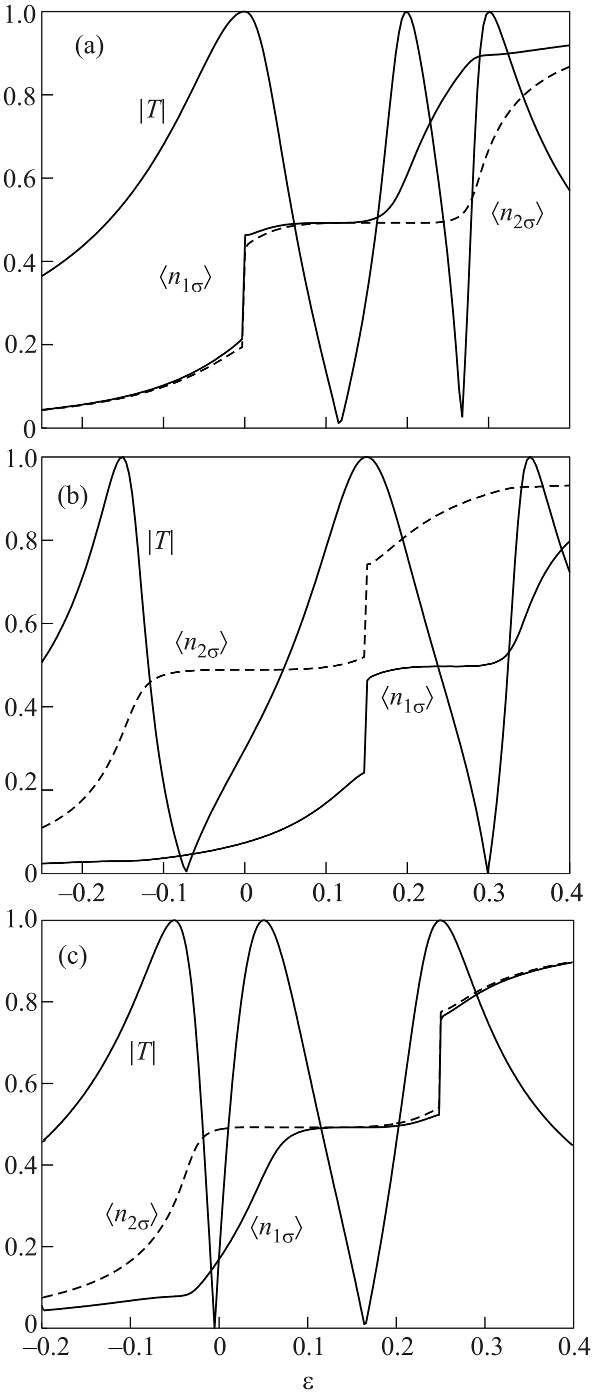


Fig.3. The electron populations as dependent on the energy of incident electron defined by (8) for the parameters of the system given in Fig.1. (a) $\epsilon = 0$, (b) $\epsilon = -0.15$, and (c) $\epsilon = -0.05$

Since the resonance width turns to zero with approaching the BIC point, we expect singular behavior of occupation numbers (8) at the energy of BIC. In fact, Fig.3a, b, c demonstrate this effect. Let us consider the first BIC at $\epsilon = 0$ with discrete energy $E = 0$ at which the single-electron energies in QD are crossing as shown

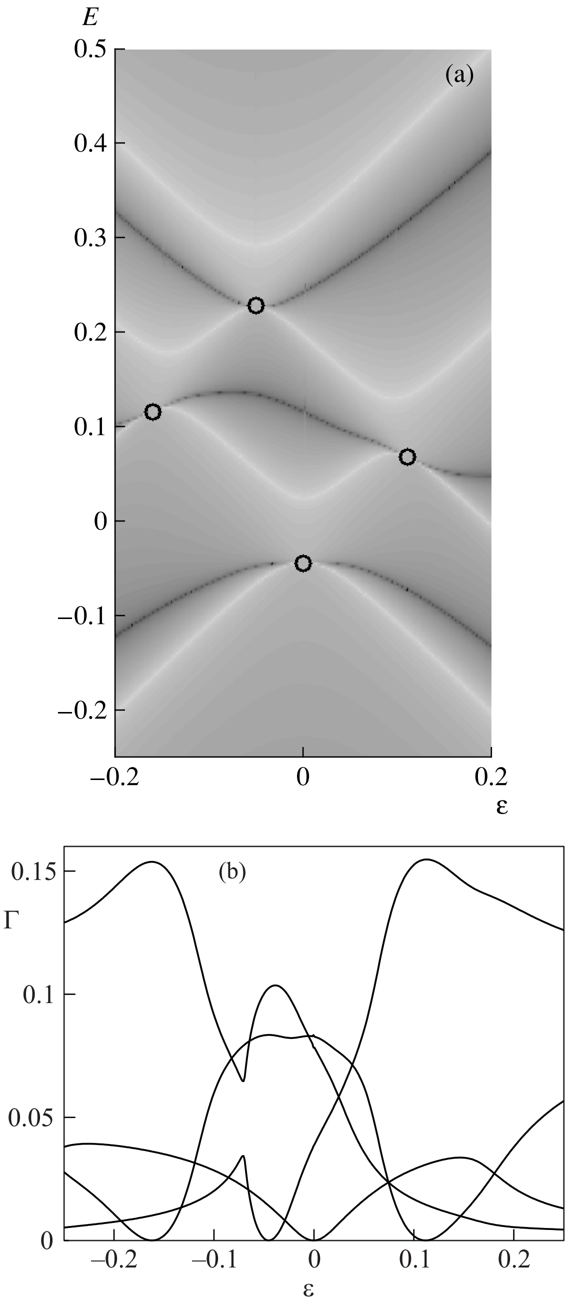


Fig.4. (a) The transmission $\ln(-\ln(1-|T|))$ of QD versus energy of incident electron and energy splitting $\epsilon$ in the avoiding crossing scenario $v = 0.05$, $U_1 = 0.2$, $U_2 = 0.3$, $\Gamma_1 = \Gamma_2 = 0.05$. Black regions correspond to those where the transmission close to zero while the white ones do to those where the transmission is near unit. Thereby the white regions follow the single-electron and two-electron energy levels in closed QD. Positions of BICs are shown by open circles. (b) The resonance widths as shown in Fig.2b, but in the avoiding crossing scenario

in Fig.1b. One can see from Fig.3a that at the energy $E = 0$ both energy levels are sharply and simultaneously populated till one half. The next resonances with finite

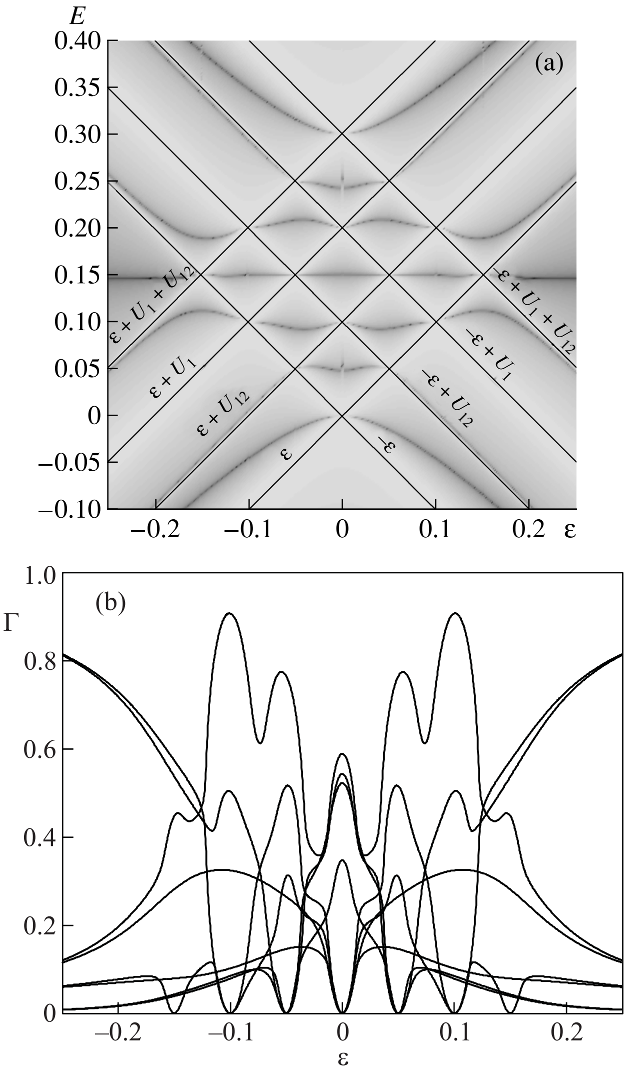


Fig.5. The same as in Fig.4 but with inclusion of the inter-level Coulomb interactions $U_{12} = 0.1$.(a) The transmission $\ln|T|$ of QD versus energy of incident electron and energy splitting $\epsilon$ in the avoiding crossing scenario $v = 0.05$, $U_1 = U_2 = 0.2$, $\Gamma_1 = \Gamma_2 = 0.1$. (b) The resonance widths defined as $-2\mathrm{Im}[z_\lambda(E,\epsilon)]$, $\lambda = 1, 2, \ldots 8$ versus $\epsilon$ for $E = 0$ where $z_\lambda$ are the poles of the Green function (10)

widths correspond to the two-electron energies of QD that are populated smoothly at the Hubbard repulsive energies $U_1 = 0.2$ and $U_2 = 0.3$ by usual scenario as seen from Fig.3a.

The next BICs happen for the single-electron state crosses the two-electron state at points $\epsilon = -0.15$ and $\epsilon = 0.1$. Because of similarity of these BIC points we have presented here only the first case as shown in Fig.3b. The BIC's discrete energy for that case equals to $E = 0.15$ (Fig.1). Again we see that for approaching to this energy the BIC populates sharply. However the populations of the single-electron level and two-electron one are well separated because of the Hubbard repulsion of the two-electron state. The last figure Fig.3c refers to the crossing of two-electron energies at the point $\epsilon = -0.05$. As seen from Fig.1a the two-electron BIC has energy $E = 0.25$. As a result for approaching this energy we observe sharp population of this state similar to the case (a).

Are BICs critical to energy level crossing? Similar to [9, 12] we lift the degeneracy in the QD by transitions between levels, adding a hopping term between the single-electron states into the Hamiltonian of the two-level QD, $H_D \to H_D - va^+_{1\sigma}a_{2\sigma} - va^+_{2\sigma}a_{1\sigma}$ which evolves the picture of energy crossing into a picture with an avoided crossing. Fig.4a shows the transmission of QD in which the energy levels repel each other because of the hopping between QD levels. In order to show clearly the zero and unit transmission we present the transmission in the double log scale $\ln(-\ln(1-|T|))$. One can see the avoided level crossings shown by white lines with $T = 1$. BICs shown by open circles are located at those points where the unit transmission $T = 1$ (white lines) crosses the zero one $G = 0$ (black lines) similar to the case of non interacting electrons [12]. Fig.4b shows that the resonance widths turn to zero at four critical values of $\epsilon$.

The Hubbard repulsion presented in the Anderson impurity model (3) is not the only way to account the Coulomb interactions. The last also induce the inter-level couplings in the form $\sum_{mn}\sum_{\sigma\sigma'} U_{mn}n_{m\sigma}n_{n\sigma'}$. Therefore, in the two-level approach a new Coulomb constant $U_{12}$ appears. The equations of motion for the Green functions in the QD become tedious but still complete to give the following Green function

$$G_{QD,m\sigma}(E) = \\ = \frac{(E+E_m)(E+E_m-U_m-U_{12}\langle n_{\overline{m}\sigma}\rangle)(E+E_m-U_{12}-U_m\langle n_m\rangle)}{(E+E_m-U_m(1-\langle n_{m\sigma}\rangle)-U_{12}\langle n_{\overline{m}\sigma}\rangle)(E+E_m-U_{12}(1-\langle n_{\overline{m}\sigma}\rangle)-U_m\langle n_{\overline{m}\sigma}\rangle)(E+E_m-U_m-U_{12}\langle n_{\overline{m}\sigma}\rangle)}, \quad (10)$$

where $m = 1, 2$, $\overline{m} = 2, 1$, $E_m = \mp\epsilon$. A substitution of (10) into Eqs. (5), (8) and (9) allows to calculate the transmission of the QD presented in Fig.5a. Each crossing of energy levels shown by solid lines gives rise to BICs as shown in Fig.5b. One can see that for $\epsilon = 0$ there are simultaneously four crossings. As a result at this points four resonance width turn to zero as shown in Fig.5b. Corresponding at the points $\epsilon = \pm 0.05$ we obtain three BICs and so on. If to compare all Figures with transmission probability through the QD one can see that the Coulomb interactions in QD replicate the transmission zeros which are between neighboring resonances. If the resonances are crossing by an effect of gate voltage we observe BICs at each crossing points [6] as Figs.2, 4b and 5b show.

AF thanks Igor Sandalov for helpful discussions.


1. J. von Neumann and E. Wigner, Phys. Z. **30**, 465 (1929).
2. F. H. Stillinger and D. R. Herrick, Phys. Rev. A **11**, 446 (1975).
3. D. R. Herrik, Physica B **85**, 44, 270 (1977).
4. F. H. Stillinger, Physica B **85**, 270 (1977).
5. F. Capasso et al., Nature (London) **358**, 565 (1992).
6. H. Friedrich and D. Wintgen, Phys. Rev. A **32**, 3231 (1985).
7. T. V. Shahbazyan and M. E. Raikh, Phys. Rev. B **49**, 17 123 (1994).
8. S. Fan, P. R. Villeneuve, J. D. Joannopoulos, and H. A. Haus, Phys. Rev. Lett. **80**, 960 (1998).
9. A. Volya and V. Zelevinsky, Phys. Rev. C **67**, 054322 (2003).
10. M. L. Ladron de Guevara, F. Claro, and P. A. Orellana, Phys. Rev. B **67**, 195335 (2003).
11. I. Rotter and A. F. Sadreev, Phys. Rev. E **69**, 066201 (2004); ibid **71**, 046204 (2005).
12. A. F. Sadreev, E. N. Bulgakov, and I. Rotter, Phys. Rev. B **73**, 235342 (2006).
13. C. S. Kim, A. M. Satanin, Y. S. Joe, and R. M. Cosby, Phys. Rev. B **60**, 10962 (1999).
14. O. Olendski and L. Mikhailovska, Phys. Rev. B **66**, 035331 (2002).
15. G. Ordonez, K. Na, and S. Kim, Phys. Rev. A **73**, 022113 (2006).
16. E. N. Bulgakov, K. N. Pichugin, A. F. Sadreev, and I. Rotter, JETP Lett. **84**, 508 (2006).
17. E. N. Bulgakov, I. Rotter, and A. F. Sadreev, Phys. Rev. A **75**, 067401 (2007).
18. C. Texier, J. Phys. A: Math. Gen. **35**, 3389 (2002).
19. A. I. Magunov, I. Rotter, and S. I. Strakhova, J. Phys. B: At. Mol. Opt. Phys. **32**, 1669 (1999).
20. L. S. Cederbaum, R. S. Friedman, V. M. Ryaboy, and N. Moiseyev, Phys. Rev. Lett. **90**, 13001 (2003).
21. P. W. Anderson, Phys. Rev. **124**, 41 (1961).

22. Y. Meir and N. S. Wingreen, Phys. Rev. Lett. **68**, 2512 (1992).
23. H. Haug and A.-P. Jauho, *Quantum Kinetics in Transport and Optics of Semiconductors*, Springer-Verlag, Berlin, 1996.
24. H. Lu, R. Lü, and B.-F. Zhu, Phys. Rev. B **71**, 235320 (2005).
25. W. Rudziński, J. Barnaś, R. Świrkowicz, and M. Wilczyński, Phys. Rev. B **71**, 205307 (2005).
26. V. Meden and F. Marquardt, Phys. Rev. Lett. **96**, 146801 (2006).
27. P. Trocha and J. Barnaś, arXiv:0711.3611v1 (2007).
28. C. Lacroix, J. Phys. F: Metal Phys. **11**, 2389 (1981).
29. A. C. Hewson, Phys. Rev. **144**, 420 (1966).